Nonlinear Inverse Reconstruction for Real-Time MRI of the Human Heart Using Undersampled Radial FLASH

Martin Uecker,* Shuo Zhang, and Jens Frahm

A previously proposed nonlinear inverse reconstruction for autocalibrated parallel imaging simultaneously estimates coil sensitivities and image content. This work exploits this property for real-time MRI, where coil sensitivities need to be dynamically adapted to the conditions generated by moving objects. The development comprises (i) an extension of the nonlinear inverse algorithm to non-Cartesian *k*-space encodings, (ii) its implementation on a graphical processing unit to reduce reconstruction times, and (iii) the use of a convolution-based iteration, which considerably simplifies the graphical processing unit implementation compared to a gridding technique. The method is validated for real-time MRI of the human heart at 3 T using radio frequency-spoiled radial FLASH (pulse repetition time/echo time = 2.0/1.3 ms, flip angle 8°). The results demonstrate artifact-free reconstructions from only 65–85 spokes, with 256 oversampled data points. Acquisition times of 130–170 ms resulted in 29–38 frames per second for sliding window reconstructions (factor 5). While offline reconstructions required 1–2 sec, real-time applications with modified parameters and slightly lower image quality were achieved within 90 ms per graphical processing unit. Magn Reson Med 63:1456–1462, 2010. © 2010 Wiley-Liss, Inc.

Key words: inverse problems; iterative reconstruction; parallel imaging; nonlinear inversion; real-time imaging; cardiac imaging; GPU

Recently, nonlinear algorithms for improved autocalibrated parallel imaging (1,2) have been described, which combine the use of variable density trajectories with the joint estimation of image content and coil sensitivities. For the algorithm presented in Uecker et al. (2), it could also be shown that only a very small central *k*-space area with full sampling is required for accurate autocalibration. Both properties are particularly attractive for real-time imaging, where the coil sensitivity information has to be frequently updated to match the actual experimental situation generated by a moving object. A further strength of the algorithm is its inherent flexibility, which allows for arbitrary sampling patterns and *k*-space trajectories. In fact, the specific application to a radial trajectory leads to a completely self-contained reconstruction process, so that the real-time data can be processed without any special calibration of the coil sensitivities.

In order to apply a nonlinear inverse reconstruction to non-Cartesian *k*-space data, it has been proposed to add an interpolation step to each iteration of the algorithm (3). Because such computations are rather slow, one may consider the use of a graphical processing unit (GPU) to achieve reasonable reconstruction times. A corresponding implementation for iterative SENSE (4) has indeed been utilized for real-time imaging (5). However, an efficient implementation of the interpolation algorithm on a GPU is a difficult and time-consuming task. The present work therefore describes an alternative solution. The extension of our previous work (2) to a non-Cartesian radial trajectory is accomplished by only a single interpolation performed in a preparatory step, while the subsequent iterative optimization relies on a convolution with the point-spread function. Although this idea has also been proposed for iterative SENSE (6), it was not found to be faster than the interpolation technique (7). However, in terms of computational demand and in contrast to an interpolation, a convolution mainly involves two applications of a fast Fourier transform algorithm. It therefore allows for a very simple GPU implementation, which then may be exploited to realize considerable reductions of the reconstruction time. To further reduce the computational demand, a channel compression technique was implemented, which combines the data from multiple physical receive channels into a smaller number of "virtual channels" that represent their principal components.

Experimental demonstrations of the proposed method deal with real-time MRI of the human heart based on undersampled radial fast low angle shot (FLASH) acquisitions (8). The method offers robust imaging at high temporal resolution, without cardiac gating, and during free breathing.

THEORY

Regularized Nonlinear Inversion

The MRI signal equation is a nonlinear equation, which maps the unknown spin density ρ and coil sensitivities c_j to the data acquired from all receive coils

$$F : x := (\rho, c_1, \ldots, c_N) \mapsto (s_1, \ldots, s_N). \quad [1]$$

The operator is given by

$$F : x \mapsto \begin{pmatrix} P_{\tilde{k}} \mathcal{F} P_{FOV}\{c_1 \cdot \rho\} \\ \vdots \\ P_{\tilde{k}} \mathcal{F} P_{FOV}\{c_N \cdot \rho\} \end{pmatrix} \quad \text{with} \quad x = \begin{pmatrix} \rho \\ c_1 \\ \vdots \\ c_N \end{pmatrix}, \quad [2]$$

where $\mathcal{F}$ is the (multidimensional) Fourier transform, $P_{\tilde{k}}$ is the orthogonal projection onto the trajectory, and FOV is the field of view. Because the object is restricted to a

Biomedizinische NMR Forschungs GmbH am Max-Planck-Institut für biophysikalische Chemie, Göttingen, Germany

*Correspondence to: Martin Uecker, Ph.D., Biomedizinische NMR Forschungs GmbH, 37070 Göttingen, Germany. E-mail: muecker@gwdg.de

Received 25 September 2009; revised 20 January 2010; accepted 22 February 2010.

DOI 10.1002/mrm.22453

Published online in Wiley InterScience (www.interscience.wiley.com).

finite area defined by the projection P_{FOV}, the Fourier transform can be implemented with fast Fourier transform FFT algorithm after periodic extension. Solving this nonlinear equation jointly for the spin density and coil sensitivities improves the accuracy of both estimated quantities compared with traditional algorithms for autocalibrated parallel imaging (2). Moreover, because the algorithm moves most of the low frequency variations into the estimated coil sensitivities, it produces a very homogeneous image.

The solution to Eq. [1] is calculated with the iteratively regularized Gauss Newton method (9). It is applied to the operator equation modified by an additional positive definite weighting matrix $G = F \circ W^{-1/2}$. The reconstruction employs an initial guess x_0, which is improved in an iterative process by solving a regularized linearization of the signal equation. The improved estimation x_{n+1} is given in terms of the operator G, its derivative DG, and the adjoint of its derivative DG^H by the update rule

$$x_{n+1} - x_n = \left(DG_{x_n}^H DG_{x_n} + \alpha_n I\right)^{-1} \left(DG_{x_n}^H (y - Gx_n) - \alpha_n x_n\right). \quad [3]$$

The weighting matrix $W^{1/2}$ constrains the solutions of this bilinear equation to comply with prior information. It is a block matrix consisting of two submatrices: The first penalizes high frequencies in the coil sensitivities according to $(1 + a \cdot \|k\|^2)^l$ with properly chosen constants, and the second contains a regularization term for the image. Here, this term is the identity matrix, which corresponds to a conventional L_2-regularization for the image.

The regularization parameter α is reduced in each iteration according to $\alpha_n = \alpha_0 q^n$ with $q \in (0, 1)$. Thus, the regularization of the last iteration determines the tradeoff between noise and artifact in the reconstructed image. It is commonly controlled by changing the number of iterations while keeping the initial regularization α_0 fixed. As for all Newton methods, the algorithm requires a suitable initial guess. Typically, the object part is initialized to 1 and the coil sensitivities to zero. For the efficient reconstruction of a time series of images, it is advisable to use the previous frame as an initial guess in order to reduce the computation time.

Extension to Non-Cartesian Trajectories

An extension of the algorithm to non-Cartesian trajectories can be achieved by adding an interpolation (3) to the operator that performs a regridding of the k-space data. Alternatively, this work employs a technique that is similar to the convolution-based sensitivity encoding (SENSE) algorithm described earlier (6).

Starting from a continuous description, the forward operator F can be decomposed into a (nonlinear) operator C, which contains the multiplication of the object with the sensitivities, a projection P_{FOV} onto the FOV, the Fourier transformation $\mathcal{F}$, and a projection $P_{\tilde{k}}$ onto the trajectory:

$$F = P_{\tilde{k}} \mathcal{F} P_{FOV} C \quad [4]$$

Multiplication of this operator with the weighting matrix $W^{-1/2}$ and insertion of the result into the update rule for the iteratively regularized Gauss Newton method yields

$$dx = (W^{-1/2} DC_{x_n}^H P_{FOV} \mathcal{F}^{-1} P_{\tilde{k}} \mathcal{F} P_{FOV} DC_{x_n} W^{-1/2} + \alpha_n I)^{-1} \times (W^{-1/2} DC_{x_n}^H P_{FOV} \mathcal{F}^{-1} (y - P_{\tilde{k}} \mathcal{F} P_{FOV} \circ CW^{-1/2} x_n) - \alpha_n x_n). \quad [5]$$

The process takes advantage of the idempotence and self-adjointness of an orthogonal projection ($PP = P$ and $P^H = P$) and that the data y are already given on the trajectory $P_{\tilde{k}} y = y$.

As for convolution-based SENSE, the term $\mathcal{F}^{-1} P_{\tilde{k}} \mathcal{F}$ can be understood as a convolution with the point-spread function. Because this convolution only needs to be evaluated on an area with compact support as defined by the projection P_{FOV}, it can, after discretization, efficiently be implemented with the use of a fast Fourier transform on a 2-fold oversampled grid. In a preparatory step, therefore, the vector y is discretized by interpolating the data onto a grid and the point-spread function is calculated.

Preprocessing

First, a whitening step is used to decorrelate the acquired data. Starting from an eigen decomposition $U\Sigma U^H$ of the noise correlation matrix, the receive channels are transformed according to $\Sigma^{-1/2} U^H$.

Second, to reduce the computation time, a principal component analysis is applied to the data of the first frame. Only the first principal components are then used for the reconstruction process. This is a standard technique from multivariate analysis and known as array compression in the context of MRI (8,10). Given an eigen decomposition $U\Sigma U^H$ of the covariance matrix of the data, the receive channels are transformed according to U^H. From these virtual channels, only a subset corresponding to the highest eigenvalues is used for reconstruction.

The above processing steps linearly recombine the physical receive channels to fewer virtual channels. Because the coil sensitivity estimation is integrated into the nonlinear reconstruction, no further changes are necessary. The algorithm simply estimates the virtual sensitivities of the transformed channels instead of the physical sensitivities.

As a final preprocessing step, the data are interpolated onto a Cartesian grid. However, in contrast to the conventional gridding technique, no density compensation has to be used.

The complete data flow of the reconstruction process is summarized in Fig. 1.

MATERIALS AND METHODS

Data Acquisition

Real-time MRI of the heart of healthy human subjects was performed at 3 T (Siemens Magnetom TIM Trio, Erlangen, Germany) with the use of radiofrequency-spoiled radial FLASH (pulse repetition time/echo time = 2.0/1.3 ms, flip angle 8°). All acquisitions were performed without cardiac gating and during free breathing. Informed written consent was obtained from all subjects prior to the examination.

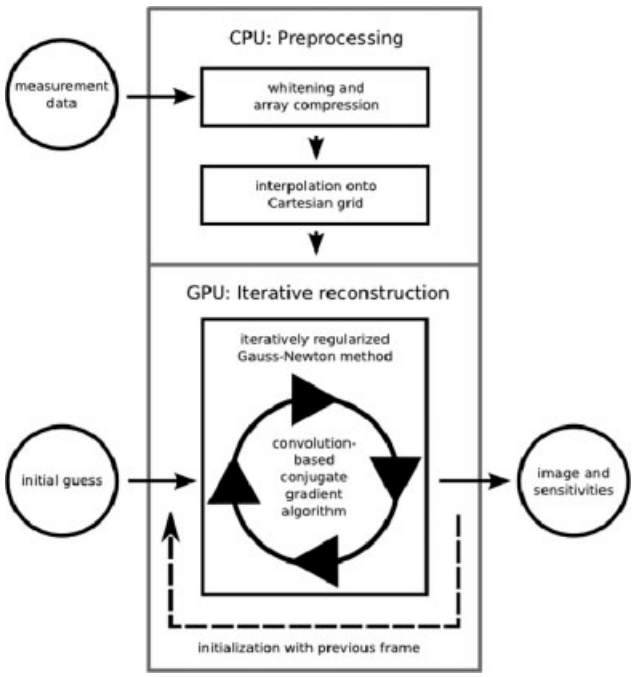

FIG. 1. Flow diagram for nonlinear inverse reconstructions from non-Cartesian encodings using a GPU. For details see text.

The images covered a 256×256 mm^2 FOV with a variable number of spokes. Each spoke had a base resolution of 128 data points, which led to 256 complex samples, for a 2-fold oversampling. To avoid any aliasing of body parts that are outside the FOV, the actual computations were performed after interpolation to an oversampled 384×384 grid, and the resulting images were cropped for display purposes. All images had an in-plane resolution of 2 mm and a slice thickness of 8 mm.

The data were acquired with a 32-channel body array coil consisting of an anterior and posterior 16-element array. These signals were compressed to 12 virtual channels, using a principal component analysis. Real-time MRI series were obtained for radial images with 45, 65, 85, 105, and 125 spokes, respectively. The corresponding image acquisition times ranged from 90–250 ms. Because the acquisition scheme involved a five-turn interleaved view reordering, it conveniently offered the application of a sliding window reconstruction with five interleaves (8). The corresponding movies yielded rates of 20–55 frames per second.

Online reconstruction and immediate display of real-time images were accomplished with a simple gridding technique, which for images with less than 125 spokes lead to streaking artifacts of increasing strength. After data acquisition, the raw data were transferred to a different computer for offline reconstruction with the proposed nonlinear inverse algorithm.

Parameter Choice

The data vector was scaled to 100.0 in the L^2 norm after interpolation to the Cartesian grid. The regularization term for the coil sensitivities was $(1.0 + 225.0 \cdot \|k\|^2)^{16}$ for $k \in [-0.5, 0.5]$. If not mentioned otherwise, the initial regularization was set to $\alpha_0 = 1.0$ and reduced by a factor of 0.5 in each Newton step. The number of Newton steps was set to 8. In each Newton step, the conjugate gradient algorithm was stopped when the residual was reduced by a factor of 0.01. Apart from the number of Newton steps, which determines the final regularization, these generic parameters have been used without further modification in many imaging scenarios, including applications of the algorithm to both Cartesian and non-Cartesian data.

Implementation on a GPU

The main algorithm was implemented on a GPU, which is a massively data-parallel processor. In this work, two GTX 285 GPUs (Nvidia, Santa Clara, CA) were used, each providing 240 processing cores. Efficient programming of the GPU was considerably facilitated by the choice of a convolution-based algorithm. Thus, apart from the few CPU-based preprocessing and initialization steps, the GPU-based iterative optimization simplified to (i) pointwise operations, (ii) fast Fourier transform applications, and (iii) calculations of scalar products. Each of these operations is either easy to implement or readily available through the programming library of the GPU vendor. Because the interpolation of a gridding technique is difficult to implement on a GPU but not time critical, it was executed on the CPU during preprocessing.

Real-Time Reconstruction

The original idea of this work was to complement online gridding reconstructions of real-time MRI data with offline

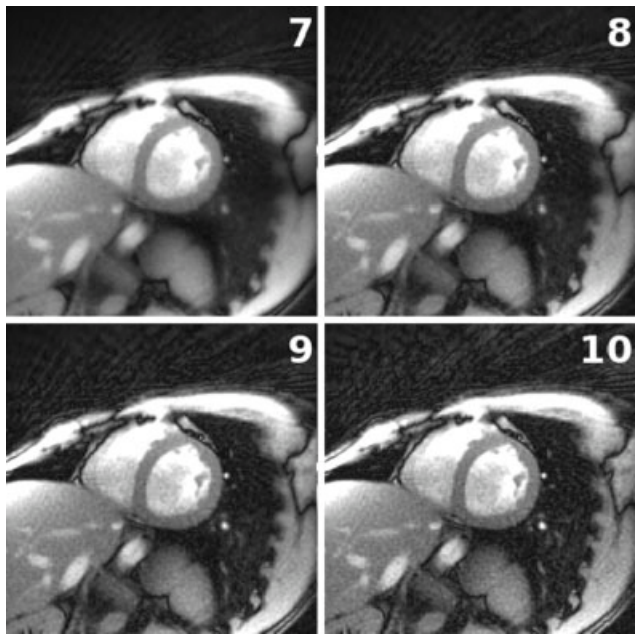

FIG. 2. A single frame from a real-time MRI data set of the human heart (short-axis view) acquired with 65 spokes per frame (3 T, radio frequency-spoiled radial FLASH, 128 data points per spoke, 2-fold oversampling to 256 complex samples, pulse repetition time/echo time = 2.0/1.3 ms, 8° flip angle). The nonlinear inverse reconstructions were obtained with a different degree of regularization using seven to 10 Newton steps.

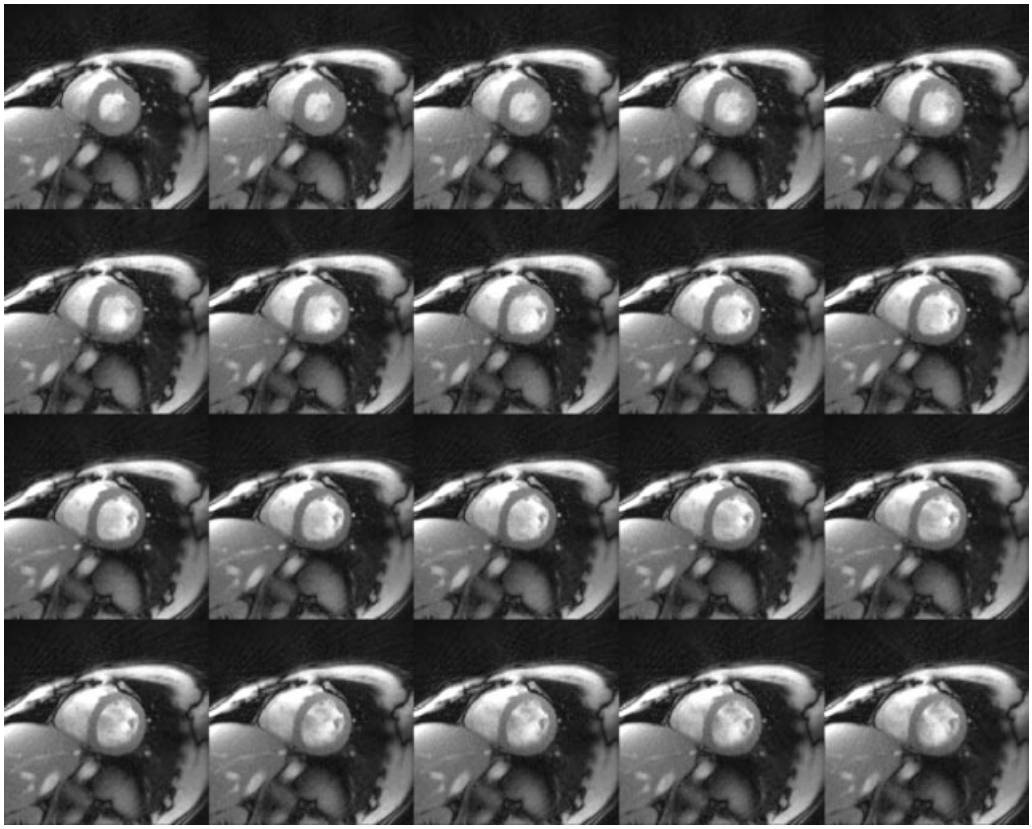

FIG. 3. Twenty consecutive frames from a real-time MRI data set of the human heart, acquired with 85 spokes per frame and reconstructed with nonlinear inversion using eight Newton steps. For other parameters, see Fig. 2.

nonlinear inverse reconstructions that offer better image quality for radial data sets with more pronounced undersampling, that is, higher frame rates. However, during the course of the study it turned out that true real-time applications of the method are already possible, although still with compromises in reconstruction quality.

To achieve real-time performance, various changes to the reconstruction process had to be made. First, the array compression of the original data was limited to the strongest six instead of 12 principal components. Second, during iterative optimization, the size of the oversampled data matrix was reduced as much as possible (from 384×384 to 256×256) to cover the FOV without too much aliasing. And third, the number of Newton steps was set to 1 and the IRGNM was initialized with the reconstruction of the previous frame. Because the regularization was no longer controlled by the number of Newton steps, the value of α_0 was set to 0.0078, as normally used for the 8th Newton

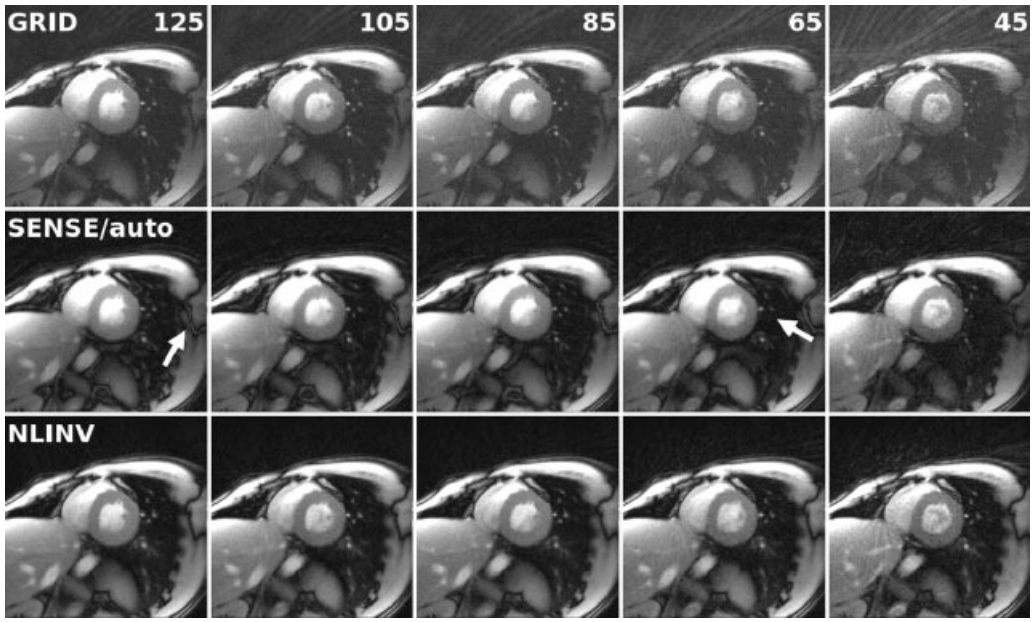

FIG. 4. A single time frame from a real-time MRI data set of the human heart during systole reconstructed by gridding (GRID), autocalibrated SENSE (SENSE/auto), and nonlinear inversion (NLINV). The reconstructions were obtained with 125 to 45 spokes per frame. Arrows indicate reconstruction artifacts (see text). For other parameters, see Fig. 2.

step. While the reconstruction becomes a linear process, a nonlinear update of the coil sensitivities was still achieved after the reconstruction of several successive frames.

With these measures, the reconstruction time could be reduced from 1–2 sec to about 90 ms per frame and GPU. Of course, such changes impair the optimum performance of the algorithm and affect the achievable image quality.

RESULTS

The influence of the regularization on the nonlinear inverse reconstruction as given by the number of Newton steps is shown in Fig. 2 for a data set with 65 spokes per frame. While only few Newton steps may lead to blurring, higher numbers or smaller regularization parameters introduce more noise. Based on these observations, all subsequent reconstructions were obtained with eight Newton steps. Corresponding results are shown in Fig. 3 for a data set with 85 spokes. The series of 20 consecutive frames at a temporal resolution of 34 ms corresponds to a total duration of 0.68 sec and a frame rate of 29 Hz (sliding window factor 5, $85/5 = 17$ spokes per image update, pulse repetition time = 2.0 ms). The short-axis views cover a single heartbeat from about peak systole (top left) to the diastolic phase (lower right).

Figure 4 compares the performance of the nonlinear algorithm to reconstructions obtained by gridding and autocalibrated SENSE. For a moderately undersampled but still relatively high number of spokes such as 125, the gridding reconstruction presents without visible streaking artifacts. Nevertheless, the images are slightly more noisy than the nonlinear reconstruction, which combines the data from all receive channels with correct phases. On the other hand, for lower numbers of spokes the gridding reconstruction cannot avoid streaking artifacts, which are mostly suppressed in the nonlinear reconstruction. For SENSE, the coil sensitivities were obtained from the densely sampled *k*-space center by reconstructing low-resolution images for each coil and dividing them by the square root of the sum-of-squares image (11). Although this approach offers visible improvements with respect to gridding, a closer inspection reveals various problems (Fig. 4, arrows): (i) local signal cancellation and the occurrence of banding artifacts, (ii) spurious signals in the background of the images, and (iii) a severe loss of detail for lower number of spokes. In constrast, the nonlinear reconstructions are free from these artifacts. If the number of spokes per frame decreases to values below 45, the quality of the nonlinear reconstruction starts to deteriorate.

The temporal resolution and, to a certain degree, the temporal fidelity of the real-time MRI acquisitions is improved by reducing the number of spokes per frame. The effect is examined in Fig. 5, which illustrates the temporal evolution (horizontal axis: 5-sec period corresponding to about five heartbeats) of a single line through a short-axis heart image (vertical axis) for reconstructions from a different number of spokes. The individual traces were obtained from 100 frames (125 spokes, 50-ms resolution), 144 frames (105 spokes, 42-ms resolution), 188 frames (85 spokes, 34-ms resolution), 233 frames (65 spokes, 26-ms resolution), and 277 frames (45 spokes, 18-ms resolution) and scaled to equal size in the temporal dimension. The image

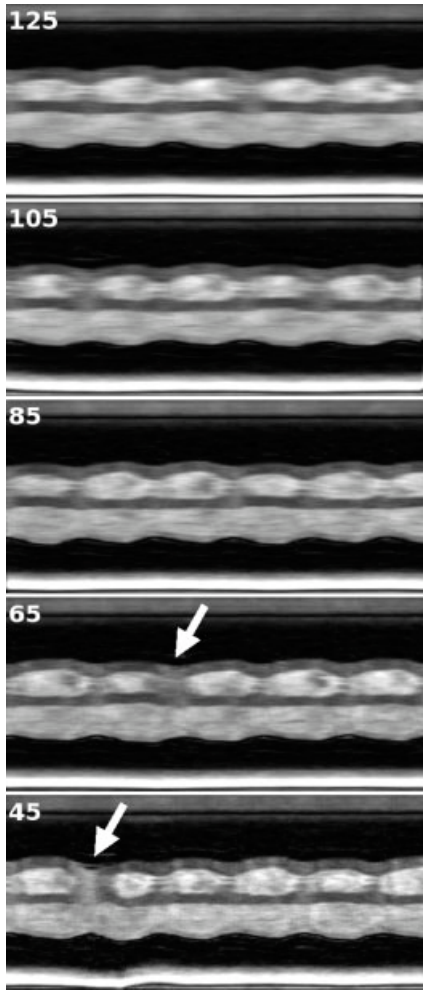

FIG. 5. Temporal evolution (horizontal axis: 5-sec period comprising five heartbeats) of a horizontal line through a short-axis view of the heart, slightly above the liver (vertical axis, compare Figs. 2 to 4). The traces refer to frames reconstructed from 125 to 45 spokes. The corresponding decrease of the acquisition time from 250 ms to 90 ms improves the visualization of the contraction and thickening of the myocardial walls (darker bands) by reducing the degree of temporal blurring. Arrows indicate intensity changes due to breathing. For other parameters, see Fig. 2.

line cuts horizontally through a cardiac short-axis view, as shown in Figs. 2–4 in a position slightly above the liver. The darker bands in Fig. 5 therefore represent the contraction and thickening of the myocardial walls, which appear less blurred for shorter image acquisition times. Larger-intensity distortions, which are also best seen in the traces derived from acquisitions with only 65 or 45 spokes (arrows in Fig. 5), are due to breathing, which leads to body movements perpendicular to the image section and corresponding disturbances of the in-plane steady-state MRI signal.

Finally, Fig. 6 compares the achievable image quality for an acquisition with 65 spokes when using a gridding reconstruction, a nonlinear inverse reconstruction, and a nonlinear inverse reconstruction modified for real-time reconstruction speed, respectively. For the currently implemented conditions, and if the sliding window is turned off,

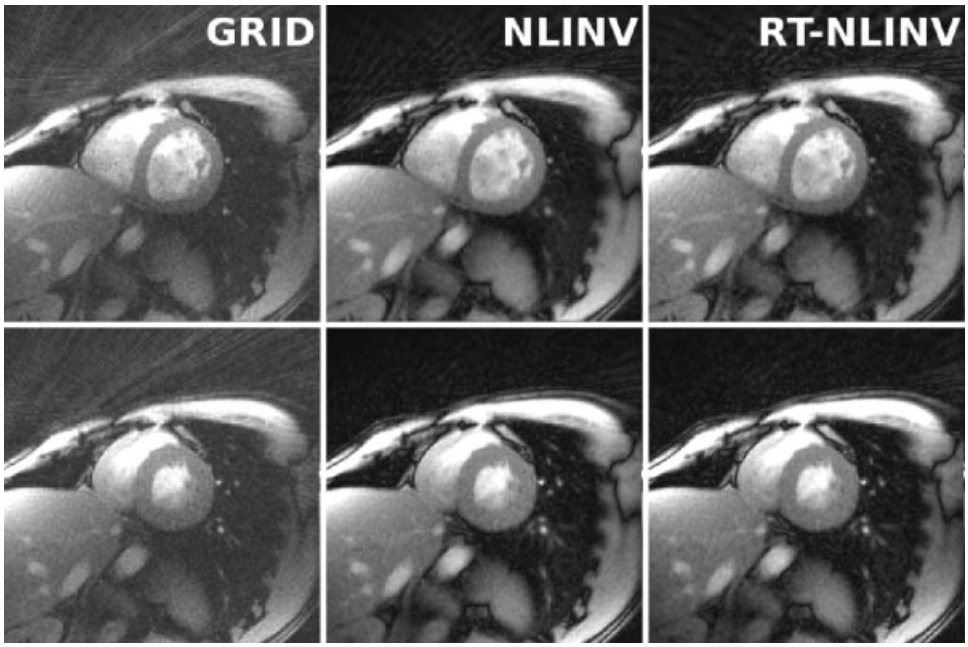

FIG. 6. Two frames from a real-time MRI data set of the human heart during (top) diastole and (bottom) systole. The images were acquired with 65 spokes and reconstructed using gridding (GRID), nonlinear inversion (NLINV), and nonlinear inversion modified to achieve real-time reconstruction speed (RT-NLINV). For other parameters, see Fig. 2.

the reconstruction time of 90 ms per frame and GPU corresponds to a frame rate of about 20 Hz for two GPUs, which in many cases is fast enough for a true real-time application. Although the real-time version of the nonlinear inverse reconstruction is somewhat degraded in comparison to the offline reconstruction, it is still superior to the gridded image, which shows more pronounced streaking artifacts.

DISCUSSION

Because of its ability to accurately estimate coil sensitivities and image content from a single acquisition with only a very small area in the central *k*-space yielding sufficient sampling density, our nonlinear inverse reconstruction for autocalibrated parallel imaging (2) emerges as an ideal choice for real-time MRI with radial trajectories. The present results for real-time MRI of the human heart fully confirm the expectations with respect to image quality and currently achievable reconstruction speed.

For radial imaging, reconstructions by self-calibrated SENSE that estimate coil sensitivities from the *k*-space center are also possible (12). Unfortunately, the method is mathematically not exact and has previously been shown to cause errors in the Cartesian case (1,2). While radial imaging is inherently more robust, a less optimal calibration of coil sensitivities may nevertheless affect the achievable image quality, which particularly holds true for applications with a higher degree of undersampling. For serial image acquisitions, the situation may be ameliorated by combining data from multiple time frames (13), provided the coil sensitivities change only slowly. In practice, however, the frequent, if not permanent, generation of new experimental conditions is an inherent property of real-time MRI studies monitoring dynamic processes. Such changes in coil sensitivities may be due to extensive organ movements (e.g., of joints such as the knee) or, in interventional MRI, be caused by the positioning of a surgical instrument or the interactive alteration of an imaging parameter. The proposed algorithm avoids these problems by jointly reconstructing image and coil sensitivities for each frame in a completely self-contained process.

The adaptation of the algorithm to non-Cartesian data by a convolution with the point-spread function separates the interpolation from the iterative optimization. The remaining part of the algorithm may therefore be accelerated by a GPU implementation, using a code that is nearly identical to that required for Cartesian data. Here, the convolution-based implementation on a GTX285 GPU achieves approximately the same speed of 1 ms per iteration and coil (384×384 processing matrix) as the approach presented in Sørensen et al. (5) (256×256 matrix). With similar performance, the main advantage of the convolution approach compared to the interpolation technique is the greatly simplified GPU implementation.

At this stage of development, the present work describes a proof-of-principle application of a real-time MRI reconstruction with frame rates of about 20 Hz. While further technical progress is foreseeable, compromises had to be made with respect to the real-time performance of the nonlinear inverse reconstruction, even when using two GPUs. First, the quality of the reconstructed images is degraded due to a lower number of virtual channels and the reduced oversampling, although the resulting image quality appeared to be acceptable for all cases studied so far, that is, for real-time cardiac MRI of a few healthy subjects. And second, the adaptation of the real-time version of the algorithm to sudden changes of the coil sensitivities is impaired because of the restriction to only one Newton step per frame. Further advances in the algorithm, its GPU implementation, and the reconstruction hardware should allow for a gradual removal of these limitations in the near future.

This study entirely focused on the principal applicability and usefulness of the nonlinear inverse reconstruction method for real-time MRI. Its success primarily relies on

a combination of (undersampled) radial encodings, the concept of parallel imaging, and its extension to a joint estimation of coil sensitivities and image content. As far as the achievable image quality is concerned, the present results may be even further improved by exploiting frame-to-frame temporal redundancies, which are inherently contained in a dynamic image series of the beating heart. Such ideas have previously been shown to improve the reconstruction quality of linear algorithms (13–16) and will be the subject of future work.

REFERENCES

1. Ying L, Sheng J. Joint image reconstruction and sensitivity estimation in SENSE (JSENSE). Magn Reson Med 2007;57:1196–1202.
2. Uecker M, Hohage T, Block KT, Frahm J. Image reconstruction by regularized nonlinear inversion: application to autocalibrated parallel imaging. Magn Reson Med 2008;60:674–682.
3. Knoll F, Clason C, Uecker M, Stollenberger S. Improved reconstruction in non-Cartesian parallel imaging by regularized nonlinear inversion. In Proceedings of the ISMRM 17th Annual Meeting, Honolulu, 2009; p. 2721.
4. Pruessmann KP, Weiger M, Scheidegger MB, Boesiger P. SENSE: sensitivity encoding for fast MRI. Magn Reson Med 1999;42:952–962.
5. Sørensen TS, Atkinson D, Schaeffter T, Hansen, MS. Real-time reconstruction of sensitivity encoded radial magnetic resonance imaging using a graphics processing unit. IEEE Trans Med Imag 2009;28:1974–1985.
6. Wajer F, Pruessmann KP. Major speedup of reconstruction for sensitivity encoding with arbitrary trajectories. In Proceedings of the ISMRM 9th Annual Meeting, Glasgow, Scotland, 2001; p. 767.
7. Eggers H, Boernert P, Boesiger P. Comparison of gridding- and convolution-based iterative reconstruction algorithms for sensitivity-encoded non-cartesian acquisition. In Proceedings of the ISMRM 10th Annual Meeting, Honolulu, 2002; p. 743.
8. Zhang S, Block KT, Frahm J. Magnetic resonance imaging in real time: advances using radial FLASH. J Magn Reson Imaging 2010;31:101–109.
9. Bakushinsky AB, Kokurin MYu. Iterative methods for approximate solution of inverse problems. Dordrecht: Springer; 2004; p. 291.
10. Buehrer M, Pruessmann KP, Boesiger P, Kozerke S. Array compression for MRI with large coil arrays. Magn Reson Med 2007;58:1131–1139.
11. Bammer R, Vigen KK, Pruessmann KP, Markl M, Moseley ME. Self-calibrating radial generalized SENSE. In Proceedings of the ISMRM 12th Annual Meeting, Kyoto, Japan, 2004; p. 2414.
12. Yeh EN, Stuber M, McKenzie CA, Botnar RM, Leiner T, Ohliger MA, Grant AK, Willig-Onwuachi JD, Sodickson DK. Inherently self-calibrating non-Cartesian parallel imaging. Magn Reson Med 2005; 54:1–8.
13. Kellman P, Epstein FH, McVeigh ER. Adaptive sensitivity encoding incorporating temporal filtering (TSENSE). Magn Reson Med 2001; 59:846–852.
14. Madore B, Glover GH, Pelc NJ. Unaliasing by Fourier-encoding the overlaps using the temporal dimension (UNFOLD), applied to cardiac imaging and fMRI. Magn Reson Med 1999;42:813–828.
15. Tsao J, Boesiger P, Pruessmann KP. k-t BLAST and k-t SENSE: dynamic MRI with high frame rate exploiting spatiotemporal correlations. Magn Reson Med 2003;50:1031–1042.
16. Xu D, King KF, Liang Z-P. Improving k-t SENSE by adaptive regularization. Magn Reson Med 2007;57:918–930.